Field-induced insulator–metal–insulator transitions in low-energy H_2^+ ion-irradiated epitaxial $La_{2/3}Ca_{1/3}MnO_3$ thin films*

Wu Zhan-Wen(伍展文)[a)b)†], Li Jie(李 洁)[a)], Li Song-Lin(黎松林)[a)], and Zheng Dong-Ning(郑东宁)[a)‡]

[a)] *Beijing National Laboratory for Condensed Matter Physics & Institute of Physics, Chinese Academy of Sciences, Beijing* 100190, *China*
[b)] *Institute of Testing and Research, Zhongshan Power Supply Bureau, Guangdong Power Grid Corporation, Zhongshan* 528400, *China*

(Received 31 January 2013; revised manuscript received 28 March 2013)

Epitaxial $La_{2/3}Ca_{1/3}MnO_3$ thin films grown on $LaAlO_3$ (001) substrates were irradiated with low-energy 120-keV H_2^+ ions over doses ranging from 10^{12} ions/cm^2 to 10^{17} ions/cm^2. The irradiation suppresses the intrinsic insulator–metal (I–M) transition temperature and increases the resistance by reducing the crystallographic symmetry of the films. No irradiation-induced columnar defects were observed in any of the samples. The specific film irradiated at a critical dose around 8×10^{15} ions/cm^2 is in a threshold state of the electric insulator where the I–M transition is absent. In an external field of 4 T or higher, the I–M transition is restored and thus an enormous magnetoresistance is observed, while a negative temperature coefficient resumes as the temperature is reduced further. Magnetic relaxation behavior is confirmed in this and other heavily irradiated samples. The results are interpreted in terms of the displacement of oxygen atoms provoked by ion irradiation and the resulting magnetic glassy state, which can be driven into a phase coexistence of metallic ferromagnetic droplets and the insulating glass matrix in a magnetic field.

Keywords: manganite, ion irradiation, magnetoresistance

PACS: 75.47.Lx, 73.43.Qt, 81.40.–z **DOI:** 10.1088/1674-1056/22/8/087503

1. Introduction

Doped perovskite manganites have attracted significant interest because the universal interactions among the charge, spin, orbital, and lattice in the systems lead to extremely rich phase diagrams. There is a physical consensus that if an e_g electron is localized at an Mn site, the symmetry of the surrounding oxygen octahedron is lowered due to the strong coupling between the electronic and elastic degrees of freedom. That is, phases with distorted MnO_6 octahedra are generally insulating, and otherwise are metallic. An energy landscape with the undistorted state the local minimum and the distorted state the global minimum has been proposed.[1] Apparently, weak external perturbations like the field, pressure, and exposure to photons such as visible light,[2] lasers,[3,4] X-rays,[5] focused electrons,[6] and even accelerated ions[7–16] can all modify the landscape, and thus induce transitions to some metastable states, giving rise to extraordinary magnetic and electric properties.

Ion irradiation or implantation can introduce a controlled degree of defects. Several kinds of ions such as Ar,[7] Cr,[8] O,[9,13] Fe,[11] Ag,[10,12,14,15] and Ga[16] of energies 100 keV–200 MeV and doses 10^{11} ions/cm^2–10^{16} ions/cm^2 have been adopted to irradiate manganites. The irradiations generally cause a shift in the insulator–metal (I–M) transition to lower temperatures, a decrease in the conductivity and an enhancement of the low-temperature magnetoresistance (MR), with only an exception in $La_{0.5}Pr_{0.2}Ba_{0.3}MnO_3$.[12] These influences have been attributed to lattice disorders, oxygen deficiency, strains, and also ion substitutions. In this experiment, we irradiated epitaxial $La_{2/3}Ca_{1/3}MnO_3$ (LCMO) thin films grown on $LaAlO_3$ (001) substrates with low-energy 120 keV H_2^+ ions over a very large dose range from 10^{12} ions/cm^2 to 10^{17} ions/cm^2. Besides the conventionally reported phenomena, a field-induced insulator–metal–insulator (I–M–I) transition was observed in a film irradiated at a critical dose 8×10^{15}. The relationship of this phenomenon to the irradiation-induced structural changes in the film has been resolved.

2. Experimental methods

LCMO thin films were grown on $LaAlO_3$ (001) (LAO) single-crystal substrates by pulsed laser deposition at 650 °C in 60 Pa oxygen ambient.[17,18] The films were epitaxial with a thickness of about 200 nm, and were then uniformly irradiated with 120 keV H_2^+ ions at doses varying from 10^{12} ions/cm^2 to 10^{17} ions/cm^2 at an angle of 7° to avoid ion channelling. As seen in Fig. 1, data simulation using SRIM2006[19] suggests that the implantation depth of the H_2^+ ions in LCMO is $\sim$ 500 nm, and therefore the whole thickness of the film is affected by ion irradiation. A few H_2^+ ions may remain in the films as interstitial impurities, while most of them rest

*Project supported by the National Basic Research Program of China (Grant No. 2011CBA00106) and the National Natural Science Foundation of China (Grant Nos. 11174342, 11161130519, and 11104333).

†Corresponding author. E-mail: iupro@163.com
‡Corresponding author. E-mail: dzheng@aphy.iphy.ac.cn

© 2013 Chinese Physical Society and IOP Publishing Ltd

in the substrate. Each of these films were carefully investigated by X-ray diffraction (XRD) and scanning electron microscopy (SEM) before and after the irradiation. The resistances were measured by the standard four-probe technique in a physical property measurement system (PPMS220), and the magnetic measurements were carried out in a superconducting magnetometer (Quantum Design), with the field applied in the film plane. Raman spectroscopy was also used to study the irradiation-induced structure modification in the films.

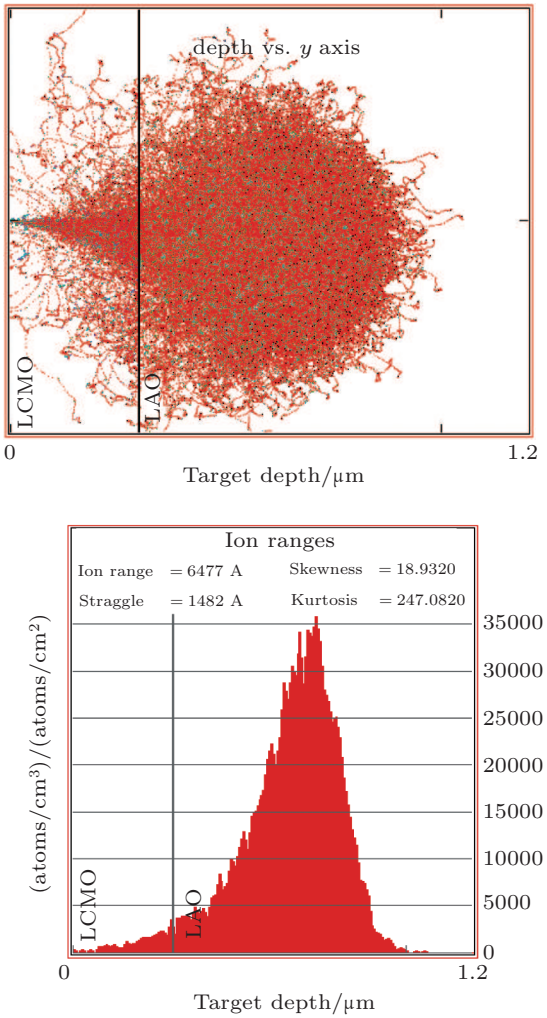


Fig. 1. (color online) The SRIM2006 data simulation results for a 300 nm thick film irradiated by 120 eV H_2^+ ions. The depth of the peak concentration is around 500 nm.

3. Results and discussion

Figure 2 shows the influence of the H_2^+ ion irradiation on the temperature dependence of the resistance (R–T) of the samples. The pristine film has the lowest room-temperature resistance, and undergoes an I–M transition at $T_P = 256$ K, similar to the bulk value. The ion irradiation causes T_P to shift to lower temperatures and the resistance to increase. The I–M transition still presents in the film irradiated at 5×10^{15} ion/cm^2, although at a rather reduced temperature and with a much higher resistance. However, as the dose is increased to 8×10^{15} ion/cm^2 or higher, the I–M transition is completely suppressed and the sample becomes semiconducting with a negative temperature coefficient in the whole temperature range. It is noted that, as depicted in the inset, a nonlinearity of R_{max}, the resistance at T_P, versus the irradiation dose has been observed. This may imply an irradiation-induced structural transformation or simply a percolation threshold around this critical irradiation dose of 8×10^{15} ion/cm^2.

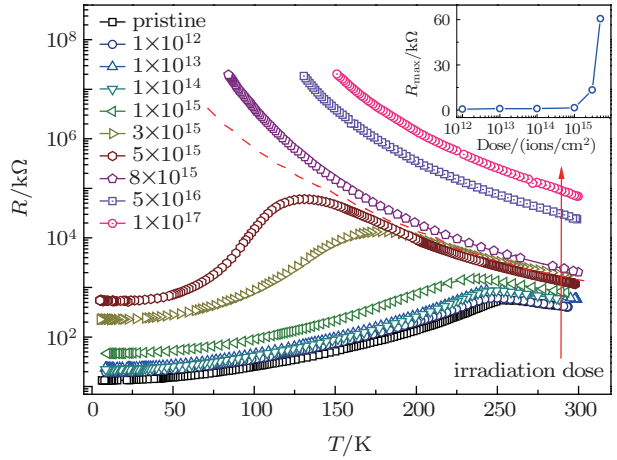


Fig. 2. (color online) R–T curves for the pristine LCMO film and films irradiated at various doses. The I–M transition disappears at a dose of 8×10^{15} ions/cm^2 or higher. Inset depicts the peak resistance as a function of the irradiation dose.

Further evidence of the structural damage due to the H_2^+ ion irradiation is given by the XRD spectra. Presented in Fig. 3 on an expanded scale are the XRD results for the films before and after irradiation. As is well known, due to the smaller size of Ca^{2+} as compared with La^{3+}, the bulk LCMO is orthorhombically distorted with the pseudocubic $(002)_c$ peak split into $(220)_o$ and $(004)_o$, mostly overlapped near 47°. Epitaxially grown on LAO substrate, the film is compressively strained to tetragonal with its (004) at 46.5°, as denoted in the pristine curve by a blue rod. If the film thickness is beyond the critical thickness of coherent epitaxial growth, generally several tens of nanometers, the misfit strain is relaxed and the orthorhombic lattice resumes. This is the reason for the observed trace of the (220) reflection (denoted by a red rod). Obviously, there are twin structures in the film. That is, domains with MnO_6 octahedra tilting towards different directions exist in the film. Ion irradiation apparently broadens the reflections, decreases their intensity, and also further separates the two peaks. This implies that upon ion irradiation, the lattice distortion is aggravated and the distortion extent becomes inhomogeneous over the whole film. In addition, both reflections shift to lower 2θ values. At the highest dose of 10^{17} ions/cm^2, the c-axis lattice parameter is as high as 3.98 Å, a striking expansion from the bulk value $\sim$3.86 Å, which is actually a sign that the lattice is swollen in volume due to the ion irradiation. In brief, X-ray observations imply that the crystallographic symmetry of the

film is reduced upon H_2^+ ion irradiation and thus the Mn^{3+}–O–Mn^{4+} bond lengths and/or bond angles are changed, leading to the change in transport properties.

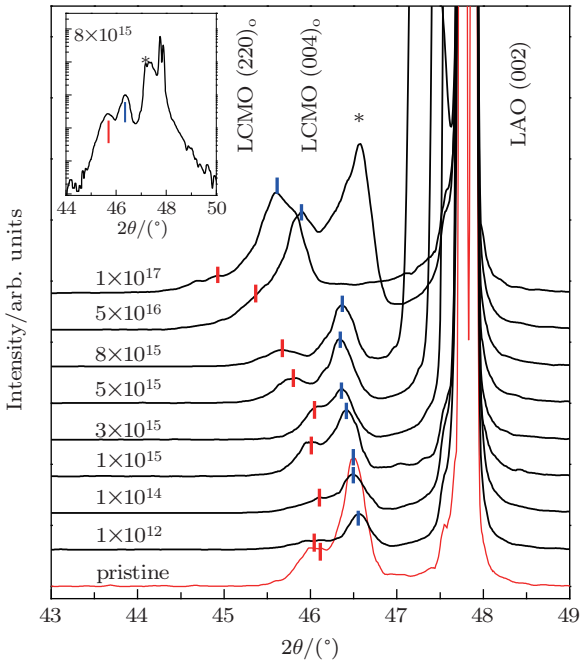


Fig. 3. (color online) The X-ray spectra on an expanded scale for the LCMO films irradiated at various doses. The red and blue rods denote the peak positions of tetragonal LCMO (220) and (004), respectively. The asterisk designates the additional reflection from the LAO substrate induced by ion irradiation. The inset is a logarithmic plot of the curve at 8×10^{15} ions/cm^2.

The curve for a dose of 8×10^{15} ion/cm^2, where the I–M transition disappears, is shown in the inset. Now the *c*-axis lattice spacing is 3.91 Å. Here we note that an additional peak appears, as labeled by an asterisk. Carefully examining the left side of the LAO (002) for doses higher than 3×10^{15}, one can observe an obvious broadening of the reflections, implying a splitting of the peak. The position of this peak also left-shifts with increasing dose and is finally isolated from the main LAO (002). A separate peak comes out at 8×10^{15} (as seen in the inset). At 5×10^{16}, the new peak corresponds to a lattice constant of 3.90 Å, much larger than the LAO bulk value 3.79 Å. One can see now that the main substrate peak is narrow again. The apparent reflection intensity enhancement of LCMO (004) at the highest dose of 1×10^{17} ions/cm^2 is actually due to a superposition on this additional substrate peak. The peak results from the ion irradiation and corresponds to a thin layer of the substrate where the implanted H_2^+ ions stay. The implanted H atoms simply make the LAO lattice expand.[16] Since the in-plane direction is basically clamped by the bulk, the out-of-plane direction expands severely. The expansion of the substrate lattice may also alter the strain status of the film, thus causing the transport property changes.

The magnetotransport properties of these irradiated films were measured in in-plane magnetic fields up to 5 T at a temperature ranges from 5 K to 300 K. Figure 4(a) shows the *R*–*T* curves of two films irradiated at 1×10^{15} ions/cm^2 and 5×10^{15} ions/cm^2, respectively, in varied magnetic fields, and figure 4(b) shows the corresponding zero-field-cooled (ZFC) MR–*H* curves measured at room temperature and 5 K, as well as at their respective I–M transition temperatures T_P: 235 K for the former and 131 K for the later. Here, three points are worthy of mention. (i) The MR value peaks around their respective T_P. No prominent low field shoulder that signifies spin-dependent tunneling across the grain boundaries is observed. This implies that although irradiated by large doses of H_2^+ ions, these films have developed no other point defects. This can also be verified by the annealing experiments afterwards. Annealed at a moderate temperature of 900 °C in 1 atm (1 atm = 1.01325×10^5 Pa) oxygen for only 6 h, the film irradiated at a very high dose of 5×10^{16} ions/cm^2 almost recovered to its pristine *R*–*T* curve, only with $T_P \sim 12$ K lower and a resistance 6 times the original value (not shown here). (ii) Ion irradiation apparently enhances the MR ratio. In the lightly irradiated sample, MR is no more than 70% in 5 T, while it reaches nearly 100% at 131 K in the heavier irradiated sample. (iii) In the lightly irradiated sample, the MR ratio shows a roughly linear dependence with the magnetic field in the heavier irradiated sample. However, a clear nonlinear behavior is recorded at 131 K, and the ZFC curve measured at 5 K manifests a clear magnetic relaxation behavior. All these suggest substantial phase transitions with the application of magnetic field in the heavier irradiated samples.

This can be further demonstrated by the specific sample irradiated at the threshold dose 8×10^{15} ion/cm^2, which reveals a remarkable MR and even experiences an I–M–I transition in external magnetic fields of 4 T or higher. Figure 5 shows the *R*–*T* curves of the sample measured in various applied fields. In a field of 2 T or below, the sample is semiconducting. At a higher field of 4 T, the film first behaves as insulating until the temperature is decreased to 76 K, where the I–M transition is reentrant. Further cooling of the sample leads to an M–I transition at 32 K, and then the temperature coefficient of the resistance retains negativity down to 2 K, revealing an insulating ground state.[16] In higher magnetic fields of 5 T and 8 T, similar I–M–I transitions are sustained, except that the sample resistance is further suppressed and the transitions are broadened. Moreover, with increasing magnetic field, the I–M transition moves to higher temperatures while the M–I transition shifts to lower temperatures, so the metallic region expands. It is important to point out that, as a comparison, we also carried out ion irradiation in $La_{2/3}Sr_{1/3}MnO_3$ (LSMO) thin films. LSMO films become insulating only after irradiation at a dose of 3×10^{16} ions/cm^2 or higher. This threshold dose value for LSMO is considerably larger than that for LCMO. Furthermore, as shown in the inset, the LSMO film irradiated at the critical dose did not show an analogous field-induced I–M–I transition. Therefore, the aforementioned observation is somewhat unique to LCMO, i.e., closely related to its electronic structure. Due to the smaller average radius of A-site ions, LCMO poses a much narrower single-electron bandwidth than LSMO.

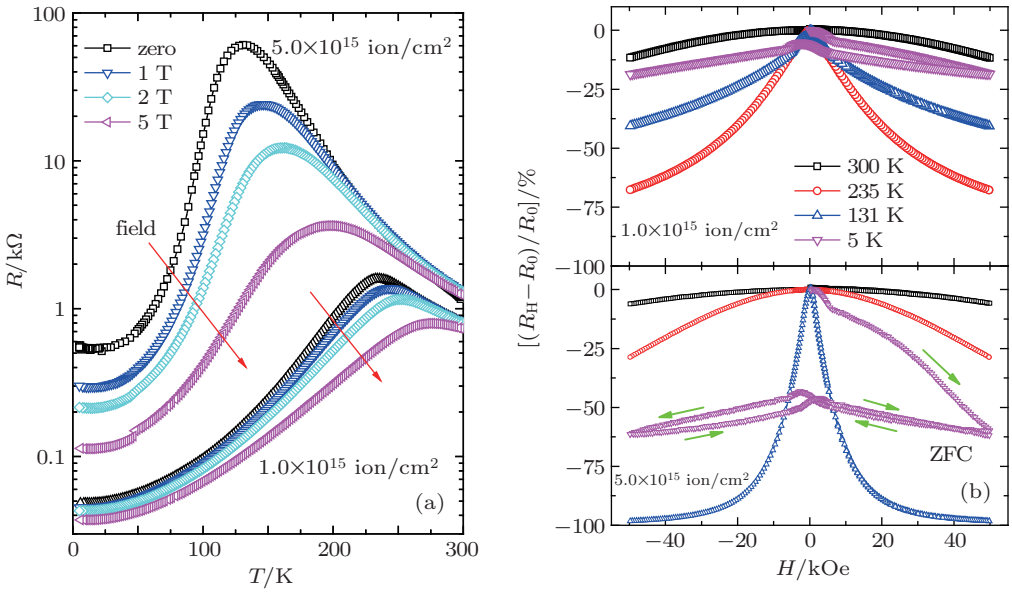


Fig. 4. (color online) (a) The *R*–*T* curves of the films irradiated at 1×10^{15} ions/cm^2 and 5×10^{15} ions/cm^2, respectively, in zero field and 1, 2, and 5 T. (b) The corresponding *MR*–*H* curves measured at 300, 235, 131, and 5 K. The unit 1 Oe = 79.5775 A·m^{-1}.

The unique magnetotransport behavior observed in the sample resembles in distorted $Eu_{0.58}Sr_{0.42}MnO_3$, in which field-induced I–M–I transitions and a spin glass (SG) ground state have been demonstrated.[20] Magnetic measurements were then performed in this ion-irradiated LCMO sample to scrutinize its magnetization properties. Figure 6(a) shows the zero-field-cooled (ZFC) and field-cooled (FC) magnetization versus temperature (*M*–*T*) curves measured in an in-plane magnetic field of 100 Oe. Apparently, by ion irradiation, the ferromagnetic transition temperature T_C determined by the Curie–Weiss law drops to $\sim$ 100 K, complying to but not exactly the same as the left-shifted T_P, meaning that there is a decoupling of T_C and T_P, which is generally observed in strained (i.e., lattice distorted) films. In addition, the ZFC curve diverges from the FC one, showing a maximum at a freezing temperature $T_f \sim 70$ K and very small magnetization values at low temperatures. This strongly suggests a magnetic glassy ground state, which may be a consequence of the competing magnetic interactions in the irradiation-induced distorted lattice structure, although an easy attribution of the state to an SG other than a cluster glass is still indiscreet. Shown in Fig. 6(b) is the *M*–*H* loop of the sample measured at 70 K after FC in 1.5 T. Since 1.5 T is not high enough to induce the I–M–I transition (see Fig. 5), the very small remanent magnetization and the unsaturation at $\pm$1.5 T confirms the glass nature of the film. However, as depicted in Fig. 6(c), at 5 K, which is well below T_f, the ZFC loop shows a larger magnetization value, a clear coercivity field, and a moderate remanent moment in a scanning field between +3 T and −3 T, suggesting the existence of a ferromagnetic (FM) phase, though the unsaturation in high fields still endorses the glass state. It is worth mentioning that the initial magnetization curve (solid line) is outside and below the hysteresis loop. This is an indication that a high magnetic field helps to align the frustrated magnetic spins and partially drive the glass insulator to an FM metal. We believe that this transition is also accompanied by a structural transformation, since an FM metal stands only in an undistorted lattice.[1] The field modifies the energy landscape of the system locally in favor of the undistorted lattice. Accordingly, the hysteresis loop measured after FC in +3 T shows an enhanced magnetization and a smaller slope in high fields. Here, in the loops the diamagnetic signal from the LAO substrate has been deducted through a linear fitting of the high field part in the 5 K loop of an LSMO film irradiated at 3×10^{16} ions/cm^2 (also shown in Fig. 5(c)). Therefore, the high field slope of the loops may be slightly underestimated.

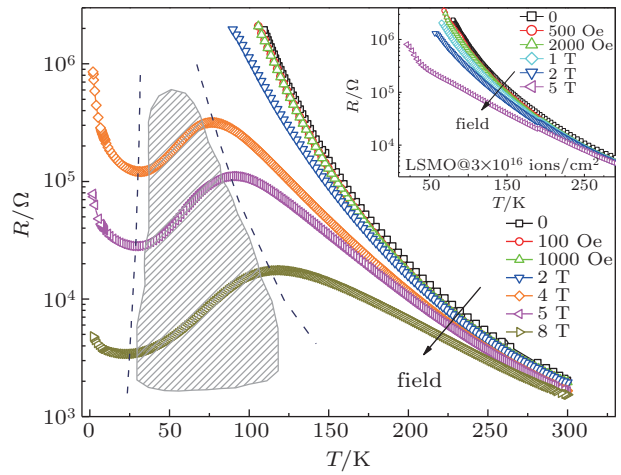


Fig. 5. (color online) The *R*–*T* curves for the LCMO film irradiated at 8×10^{15} ions/cm^2 in applied fields of 0, 100 Oe, 1000 Oe, 2 T, 4 T, 5 T, and 8 T. The field-induced metallic region in the figure is shaded. As a comparison, the *R*–*T* curves for an LSMO film irradiated at a critical dose of 3×10^{16} ions/cm^2 is depicted in the inset.

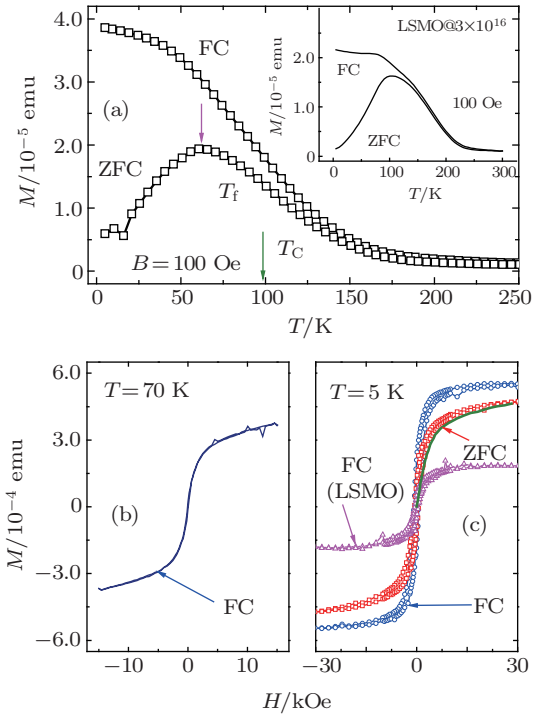


Fig. 6. (color online) (a) The FC and ZFC M–T curves, (b) the FC M–H loop at 70 K, and (c) the FC and ZFC hysteresis loops at 5 K, measured with the field in-plane for the LCMO sample at 8×10^{15} ions/cm^2. The inset shows the magnetization curves of the LSMO film irradiated at 3×10^{16} ions/cm^2. An FC hysteresis loop at 5 K for this LSMO film is also shown in panel (c).

Noting that even in the FC case, the effective magnetic moment of the sample at 5 K and 3 T is only ~ 0.75 μ_B/Mn, far below the expected saturation value of 3.6 μ_B/Mn for the FM state, it is then reasonable to claim a coexistence of field-induced FM metal and glassy insulator matrix in the sample. The metallic region shown in Fig. 5 simply originates from a percolation process of these metallic FM droplets. Nevertheless, even a field as high as 8 T cannot convert the sample completely into FM, and therefore when the temperature is further reduced, the insulating magnetic glass phase dominates, as revealed by the M–I transition in Fig. 5. The M–T measurements in high fields failed because the diamagnetic signal from the LAO substrate increases linearly with field and thus outdoes the FM signal from the film. Finally, the irradiated LSMO film also shows similar phenomena, but with much lower magnetization values. It is reasonable to conclude that the heavily irradiated LSMO film is also in a magnetic glass state, but since the state is induced in a much higher dose, it is more robust than that in LCMO. Magnetic fields cannot effectively catalyze the metallic FM phase in the LSMO film, so no field-induced I–M–I transition occurs.

Figure 7 presents the MR as a function of the applied magnetic field at different temperatures for the same sample. The curves were measured after the sample was ZFC to designated temperatures with field scanning from 0 T to +5 T and then back to −5 T; whereas the measurements at 5 K were carried out after the sample was FC in +5 T, since the ZFC resistance at 5 K is beyond the measurement range (see Fig. 5). At high temperatures, the MR values are quite limited, as shown in the left inset. Cooled down to 120 K, the value approaches 100% at 5 T, suggesting a field-induced phase transition from a high resistance state to a low resistance state, consisting of field-induced FM droplets embedded in the magnetic glass insulator. The resistance declines faster with the field and shows higher MR values at 100 K. Only trivial hystereses are observed in the curves, suggesting that at these temperatures, the glass–FM transition is reversible if the field is removed. The most striking feature is observed at 5 K, far below T_f. With the field decreasing from +5 T, the resistance first increases slowly and then upsurges near zero-field. A very sharp resistance peak with a positive MR of 120% is found at −2500 Oe, together with a remarkable hysteresis that depends on the field sweeping rate (see the short dashed line, which is from another scan). This is due to the FM–glass phase transition. At this temperature, however, the field-induced FM phase can be sustained partially even in the absence of a field, as evidenced by the remanent magnetization in Fig. 6(c). Therefore, around the coercivity field, the spin angles among the individual FM regions are at the maximum. Spin-polarized electrons are subjected to strong scattering as they tunnel across the boundaries, resulting in a remarkable resistance peak. As a supplement, the ZFC and FC MR curves for an LCMO film irradiated at a lower dose 5×10^{15} ions/cm^2 are shown in the right inset, where the relaxation to a spin ordered state in a field is clearly seen in the ZFC curve. However, in the subsequent scans the curves overlap each other since the whole film is then in an FM state.

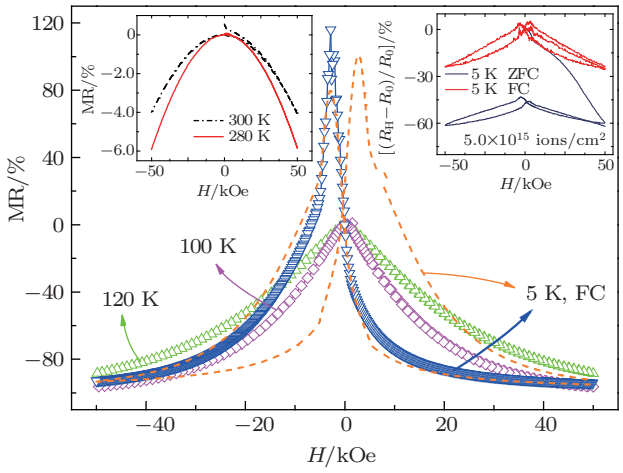


Fig. 7. (color online) MR as a function of field for the LCMO film irradiated at 8×10^{15} ions/cm^2 measured at 120, 100, and 5 K. The short dashed line is also obtained at 5 K but with a different field sweeping rate. The MR curves at 300 K and 280 K are shown in the left inset, and the right inset is the MR behavior at 5 K for an LCMO film irradiated at a lower dose of 5×10^{15} ions/cm^2.

Since the data simulation implies that almost all the accelerated H_2^+ ions traverse through the film and rest deeply in

the substrate, the observed changes in the magnetic and transport properties in the ion irradiated films are unlikely to be ascribed to a substitution of H_2^+ ions into the LCMO lattice or to H atom inclusions. The irradiation-induced lattice defects, if they exist, must be rather minor, as the annealing in 1 atmosphere oxygen at 900 °C for 6 hours can almost restore the film, especially in the case of LSMO. The surface morphology investigations by SEM also verify that no serious lattice defects, such as columnar defects,[12] have been generated in any of these ion-irradiated samples (see inset in Fig. 8), perhaps due to the very low accelerating voltage and the light mass of the ions. A slight blurring of the grain boundaries after irradiation is also observed, suggesting a very mild ion milling effect.[15] In order to further probe the underlying mechanism of the irradiation effect, a comparative Raman study (SPEX-1403, 541.5 nm) of the films was carried out and the results are presented in Fig. 8. Data from two small areas in each sample are selected and the peak positions are defined as the average value of the two curves. The peaks associated with cooperative Jahn–Teller (JT) distortion are completely absent, as previously observed in the LCMO films on LAO.[21] The bump around 500 cm^{-1}–600 cm^{-1} is due to the dynamic JT distortion related to polaron hopping. The peaks at phonon frequencies of 220.1 cm^{-1} and 435.2 cm^{-1} in the pristine film are assigned to the tilting (T) and bending (B) of the oxygen octahedra ($A_g + B_{1g}$), respectively.[21] No new phonon mode is introduced after the ion irradiation. The peak positions only shift slightly to lower frequencies, 215.5 cm^{-1} and 430.1 cm^{-1}, respectively, and their widths increase and spectral weights decrease. The softening of the tilting mode suggests a reduction in the tilt angle of the octahedra, while that of the bending mode may indicate a displacement of the O(1) atoms in the octahedra. This conclusion is consistent with the XRD results shown in Fig. 3.

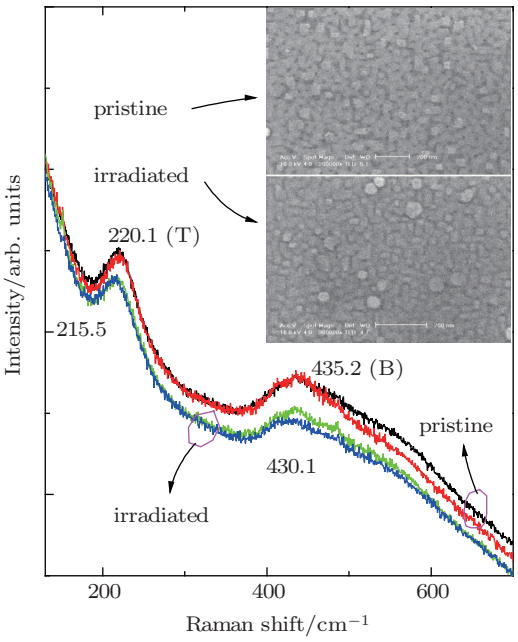


Fig. 8. (color online) Raman spectra at room temperature for the pristine LCMO film and the film irradiated at 8×10^{15} ions/cm^2. The insets are the SEM images of the films, and the scales in the images are 200 nm.

It has been reported that a reversible rhombohedral–monoclinic transition can be induced by focused electron beam irradiation in an epitaxial $La_{2/3}Sr_{1/3}MnO_3$ thin film,[6] which is referred to as a displacive transition and attributed to the displacement of oxygen atoms. In this experiment, the H_2^+ ion irradiation is roughly an energy transfer from the incident ions to the lattice, analogous to the case of electron beam irradiation, which helps to displace the oxygen atoms. A new metastable phase forms when the oxygen atoms reach their new equilibrium positions, with the crystallographic symmetry of the films reduced and the one-electron band width further narrowed. This metastable phase thus corresponds to an insulating magnetic glass state, which is stable even when ion irradiation ceases. Under a threshold state, the energy landscape of the system can be changed by a magnetic field so as to benefit the undistorted FM metal phase, leading to the unusual I–M–I transitions observed.

4. Conclusion

In summary, we studied the transport properties of $La_{2/3}Ca_{1/3}MnO_3$ thin films irradiated with 120-keV H_2^+ ions at doses from 10^{12} ions/cm^2 to 10^{17} ions/cm^2. The irradiation transfers energy to the films and thus displaces the oxygen atoms in the lattice, as well as raising the sample resistance and shifting the I–M transition peak left. As the dose is around 8×10^{15} ions/cm^2, the intrinsic I–M transition in the system disappears. Accordingly, the sample becomes insulating down to 2 K, and shows a glassy ground state. A magnetic field of 4 T or higher can partially convert the sample into an FM metal below a certain temperature. Consequently, novel I–M–I transitions and enormous MR are observed due to the percolation process in the FM phase and the spin-dependent tunneling at low temperatures across the insulating glass barriers, respectively.

Acknowledgments

The authors would like to thank Mr. Su Shao-Kui, Mr. Huang Wei-Wen, and Ms. Jia Shun-Lian for the transport measurements, and Mr. Xu Jia-Dong for performing the irradiations.

References

[1] Ahn K H, Lookman L and Bishop A R 2004 *Nature* **428** 401
[2] Hu L, Sun Y P, Wang B, Luo X, Sheng Z G, Zhu X B, Song W H, Yang Z R and Dai J M 2010 *Chin. Phys. Lett.* **27** 097504
[3] Wu D J, Wu X W and Liu X J 2006 *Chin. Phys. Lett.* **23** 1903
[4] Fiebig M, Miyano K, Tomioka Y and Tokura Y 1998 *Science* **280** 1925
[5] Kiryukhin V, Casa D, Hill J P, Keimer B, Vigliante A, Tomioka Y and Tokura Y 1997 *Nature* **386** 813
[6] Zhan Q, Yu R, He L L, Li D X, Li J, Xu S Y and Ong C K 2002 *Phys. Rev. Lett.* **88** 196104

[7] Chen C H, Talynsky V, Known C, Rajeswari M, Sharma R P, Ramesh R, Venkatesan T, Melngailis J, Zhang Z and Chu W K 1996 *Appl. Phys. Lett.* **69** 3089
[8] Cohen L F, Silva P S I P N D, Malde N, Akther Hossain A K M, Thomas K A, Chater R, MacManus-Driscoll J D, Tate T, Mathur N D, Blamire M G and Evetts J E 1998 *Appl. Phys. Lett.* **73** 1005
[9] Ogale S B, Ghosh K, Gu J Y, Shreekala R, Shinde S R, Downes M, Rajeswari M, Sharma R P, Greene R L, Venkatesan T, Ramesh R, Bathe R, Patil S I, Kumar R, Arora S K and Mehta G K 1998 *J. Appl. Phys.* **84** 6255
[10] Bathe R, Adhi K P, Patil S I, Marest G, Hannoyer B and Ogale S B 2000 *Appl. Phys. Lett.* **76** 2104
[11] Bathe R, Patil S I, Adhi K P, Hannoyer B and Marest G 2003 *J. Appl. Phys.* **93** 1127
[12] Markna J H, Parmar R N, Kuberkar D G, Kumar R, Ranaa D S and Malik S K 2006 *Appl. Phys. Lett.* **88** 152503
[13] Sirena M, Zimmers A, Haberkorn N, Kaul E E, Steren L B, Lesueur J, Wolf T, Gall Y L, Grob J J and Faini G 2010 *Phys. Rev. B* **81** 134439
[14] Choudhary R J, Kumar R, Patil S I, Husain S, Srivastava J P and Malik S K 2005 *Appl. Phys. Lett.* **86** 222501
[15] Parmar R N, Markna J H, Kuberkar D G, Kumar R, Rana D S, Bagve V C and Malik S K 2006 *Appl. Phys. Lett.* **89** 202506
[16] Pallecchia I, Pellegrino L, Bellingeri E, Siri A S, Marré D and Gazzadi G C 2008 *J. Magn. Magn. Mater.* **320** 1945
[17] Zhang M J, Li J, Peng Z H, Zheng D N, Jin A Z and Gu C Z 2006 *J. Appl. Phys.* **99** 116102
[18] Zhang M J, Li J, Peng Z H, Li S L, Zheng D N, Jin A Z and Gu C Z 2007 *J. Magn. Magn. Mater.* **316** L1
[19] Ziegler J F, Biersack J P and Littmark U 1999 *The Stopping and Range of Ions in Solids* (New York: Pergamon Press)
[20] Sundaresan A, Maignan A and Raveau B 1997 *Phys. Rev. B* **55** 5596
[21] Martín-Carrón L, Andrés A D, Martínez-Lope M J, Casais M T and Alonso J A 2002 *Phys. Rev. B* **66** 174303